

# Measurement of Shielding Effectiveness of Microwave-Protective Suits

ARTHUR W. GUY, FELLOW, IEEE, CHUNG-KWANG CHOU, SENIOR MEMBER, IEEE,  
JOHN A. McDougall, MEMBER IEEE, AND CARROL SORENSEN

**Abstract** — With more restrictive exposure standards and greater public concern about safety from nonionizing radiation, protective clothing to shield workers from dangerous levels of electromagnetic radiation has become imminently important. Tests were conducted of the shielding effectiveness of a number of microwave suits. Fabric attenuations at 10 selected locations on the suit were measured by the waveguide-transmission-loss method to evaluate the material, and relative field strengths at the surface of a full-sized phantom man model exposed to 2450-MHz free-field radiation fields with and without the suit were measured to evaluate the entire suit. The ratio of the incident power required to produce the same output from a diode *E*-field sensor placed against the synthetic tissue of the model exposed with and without the suit was used as a measure of attenuation. The waveguide measurements are important for a comparative evaluation of the different fabrics, and the free-field measurements are important for evaluating the fabric as well as the suit design and configuration in shielding effectiveness. The Navy suit provided the best performance in terms of shielding effectiveness, with attenuation varying from 34.5 to 48.7 dB, but its flammability constitutes a safety hazard. The Wave Guard suit was second best, with attenuation varying from 13.2 to 35 dB. The Milliken (20.3–33.7 dB attenuation) and Invascreen (18.7–24.5 dB attenuation) suits provide acceptable protection for *E*-field polarization parallel to the long axis of the body, but poor protection (2.0–19.2 dB for the former and 0.4–21.1 dB for the latter) for *E*-field polarization perpendicular to the body. Localized high-power-density exposures of up to 1000 mW/cm<sup>2</sup> for 1 h from a waveguide aperture did not cause material damage to any of the suit fabrics. The Milliken was the most fire retardant, but its shielding performance was the poorest, owing to the large number of openings at the pockets, cuffs, sleeves, and collar. The Invascreen suit is well designed to eliminate this problem, but the shielding of the fabric is less effective.

## I. INTRODUCTION

PROTECTIVE CLOTHING for shielding workers from dangerous levels of electromagnetic radiation has been used for many years in this country [1] and abroad [2]. Recently, increasingly restrictive standards for human exposure and greater public awareness concerning nonionizing radiation safety have resulted in a greater availability of protective clothing and the introduction of a number of new materials on the market. Most clothing of this sort consists of fabric metallized in various ways to reflect

Manuscript received December 18, 1986; revised June 4, 1987. This work was supported in part by Bell Laboratories.

A. W. Guy and C. Sorensen are with the Bioelectromagnetics Research Laboratory, Center for Bioengineering, College of Engineering, School of Medicine, University of Washington, Seattle, WA 98195.

C.-K. Chou and J. McDougall were with the Bioelectromagnetics Research Laboratory, Center for Bioengineering, University of Washington. They are now with the Division of Radiation Oncology, City of Hope National Medical Center, Duarte, CA 91010-0269.

IEEE Log Number 8716924.

incident radio-frequency (RF) energy from the wearer when exposed to high-power-density fields. Such suits would enable workers to safely approach antennas or strong radio sources for calibration or maintenance purposes without disrupting the operations. Such suits could also prove to be invaluable in protecting personnel operating high-power RF sources used for clinical treatment of patients, for example, RF hyperthermia devices for the treatment of cancer.

This paper describes tests of the effectiveness of a number of protective suits designed to shield the human body from exposure to high-intensity microwave fields. Four suits were evaluated: the Wave Guard suit used by AT&T; the suit used by the U.S. Navy; and two relatively new suits, one manufactured by the Milliken and Body Guard companies in the United States, the other manufactured by the Invertag Electronics and Telecommunication Company in Switzerland and called the Invascreen Protective System. The suits were tested on a full-scale phantom human body composed of synthetic muscle tissue enclosed in a 0.3-cm-thick fiberglass shell. The phantom body was instrumented with special diode electric-field sensors at ten different locations on the body where surface electric-field-strength measurements were made, from which the surface specific absorption rates (SAR's) of energy were determined as a function of position. These measurements were made for the model both with and without the suit while under exposure to a relatively pure plane-wave electromagnetic field at a frequency of 2450 MHz, with power densities up to 65 mW/cm<sup>2</sup>. The exposures were conducted in a large (12 ft × 24 ft × 12 ft) anechoic chamber with an absorber designed to eliminate internal reflections over a frequency range of 450 MHz through 100 GHz. The 2450-MHz fields were provided by a 10-kW klystron source.

It was originally envisioned that the suits would be tested at high levels of incident power, from 300 through 1000 mW/cm<sup>2</sup> in an anechoic chamber, but since some suit fabrics can be quite flammable, resulting in a fire hazard to the combustible absorber in the chamber, such tests were abandoned. Therefore, a simple test was devised for exposure of a portion of the fabric from the suit in a waveguide to power densities of up to 1000 mW/cm<sup>2</sup>. In addition, the flammability of each material was evaluated while in contact with an open flame.

Initial tests of suit attenuation were conducted by the waveguide-transmission-loss method. The attenuations of the suits were then determined by comparison of the measured values of SAR at the surface of the synthetic tissue of the model man when exposed with and without the suit. The surface SAR was determined by measuring the surface electric fields with a single linearly polarized dipole (diode sensor). Surface electric fields both parallel and perpendicular to the long axis of the body were measured separately at each point on the phantom tissue surface, and the total field was determined from the square root of the sum of the squares of the measured orthogonal fields. The diode sensors were calibrated by placement in an electrically thick slab of synthetic muscle tissue contained in a rectangular fiberglass box with the same wall thickness as the outer fiberglass shell thickness of the model man. Each sensor was calibrated by placing it in contact with the flat surface of the phantom tissue material while exposed to 2450-MHz radiation at normal incidence. The output voltage of the diode was measured as a function of the incident power density and compared with the SAR measured at the point of contact by temperature probes. Thus, the SAR versus output voltage of the diode was established.

Maximum sensitivity was obtained during the use of the diode sensors by modulation of the klystron source at 100 percent with a 1000-Hz square wave, and use of a Hewlett Packard (HP)-415E standing-wave ratio meter as a voltage detector. Since the meter has a narrow-band pass at 1000 Hz, it can reliably sense low-level signals with low signal-to-noise ratios. The diode-sensor meter combination allowed reliable measurements of incident field strengths as low as  $0.5 \mu\text{W}/\text{cm}^2$  at the surface of exposed tissue, corresponding to an SAR of  $0.2 \text{ mW}/\text{kg}$ . Attenuation of the suits was determined by initial exposure of the model without the suit at a relatively low power density within the range of calibration for each diode and then exposure by the model with the suit to the power density required to produce the same SAR as previously read by each diode. The ratio of input powers to the horn was recorded as the attenuation of the suit at each diode location.

## II. TECHNICAL APPROACH

### A. Characterization of Fields in Exposure Chamber

The measurements of the suit attenuations for whole-body exposure were done in the anechoic exposure chamber located in the Bioelectromagnetics Research Laboratory, University of Washington. For reasonably uniform illumination of the man model, an exposure position 458 cm from the 13.9-dB-gain Narda-644 standard-gain horn was selected. The horn was energized with a 2450-MHz amplifier set initially for an output power of 200 W and attenuated to 10 W with a directional coupler and attenuator to provide relatively low power densities in the anechoic chamber for measurement of power-density patterns both in the horizontal and in the vertical position at the exposure location. The input and reflected powers at

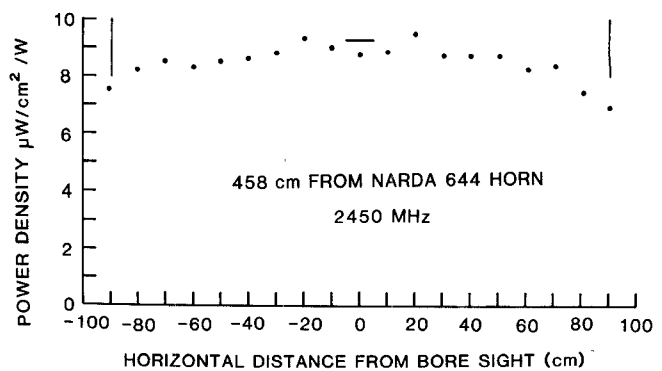


Fig. 1. Power-density pattern in horizontal plane at exposure position of the phantom model, without the presence of the model. Dots are experimental measurements, vertical lines denote positions of extreme dimensions of man when exposed in horizontal position, and the horizontal bar at the center of the graph is the theoretical power density based on the 13.9-dB gain of the horn with an input power of 1 W.

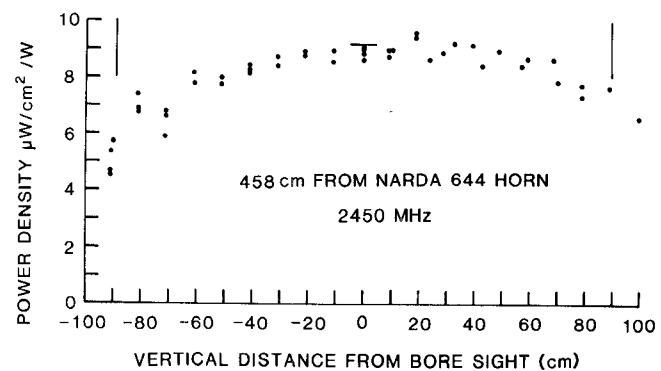


Fig. 2. Power-density pattern in vertical plane at exposure position of the phantom model, without the presence of the model. Dots are experimental measurements, horizontal lines denote positions of extreme dimensions of man when exposed in a vertical position, and the horizontal bar at the center of the graph is the theoretical power density based on the 13.9-dB gain of the horn with an input power of 1 W.

the horn were measured by HP-8484A thermistors connected to HP-435 power meters.

The power density was measured with a National Bureau of Standards EDM-1C energy-density meter. To facilitate the power-density measurement, we connected the energy-density meter directly to the probe without the cable. Thus, the meter and the probe could be easily moved in the vertical and horizontal directions in the chamber with minimum perturbations of the field. Since the meter was calibrated under conditions where the probe is connected by cable through a baffle of microwave absorber to prevent illumination of the meter, the free isolated meter reading could only be used to provide relative values of power density for definition of the radiation patterns. The absolute power density along the boresight of the horn was then properly measured with the meter, isolated from the probe by a baffle of microwave absorber, and each pattern was adjusted so that the value at the boresight corresponded to a true absolute value. Figs. 1 and 2 show the horizontal and vertical patterns of the incident power densities at 458 cm away from the horn as a function of

vertical and horizontal distance from the horn boresight. The positive coordinates correspond to the upper and right sides as seen from the horn. The power density measured at the boresight was  $9.1 \mu\text{W}/\text{cm}^2$  per watt into the horn, which is close to the theoretical value of  $9.3 \mu\text{W}/\text{cm}^2$  calculated for the 13.9-dB standard-gain horn. Power density at the most extreme distances from the boresight occupied by the man ( $\pm 89$  cm) was found to be 25 percent less than that at the boresight value. The increased deviation of power density 100 cm below the boresight compared with 100 cm above is probably due to the low-grade walk-on absorber that was used to cover the floor of the anechoic chamber. In general, the major portion of the man model was exposed to a relatively uniform far-field pattern.

### B. Fabrication of Fiberglass Man Model

A 178-cm-tall full-scale phantom model of a man was constructed. A fiberglass shell 0.3 cm thick was first fabricated around a mannequin mold, allowed to cure, and then bifurcated along the frontal plane (the back half of the shell was split from the front half) so that it could be separated from the original mold form. Detailed ears, fingers, toes, and genitalia of the man were not made. The two halves of the shell were then rejoined so as to form a complete hollow shell with the same shape as a man. The shell was then filled with synthetic gel having the same dielectric properties as human muscle tissue at 2450 MHz [3]. The completed model is shown in the exposure position in the anechoic chamber without the suit in Fig. 3. Nylon ropes passed through pulleys in the ceiling of the anechoic chamber were used to support the man with his groin area at the boresight of the transmitting horn.

### C. Design of Diode Field Detectors

A Schottky diode of the type used for standard survey meters was used as a sensing element for the electric field. An HP 5082-2810 diode sensor similar to that used in a previous study involving the measurement of SAR's in phantom models exposed to radiation from mobile antennas [4] was modified for use in this study.

The sensing element consisted of an encapsulated diode in a conducting bisected pillbox, shown in Fig. 4. The bisected pillbox formed the poles of the receiving dipole and at the same time shielded the loop formed by high-resistance-wire connections to the diode, thereby preventing any voltages from being induced by magnetic fields. The high-resistance, twisted pair, 0.001-in-diameter, 859  $\Omega/\text{ft}$ , nylon-coated resistance lead wires were protected from strain and mechanical damage by encapsulating them in a 3.2-mm (O.D.) flexible Tygon tube. The transparent high-resistance leads were made sufficiently (60–230 cm) long so that the diode could be placed at any point on the phantom man with the leads routed immediately from the front to the back of the man and then down through a connector fastened to the heel of the model. The connector was connected to miniature coaxial cables and routed to

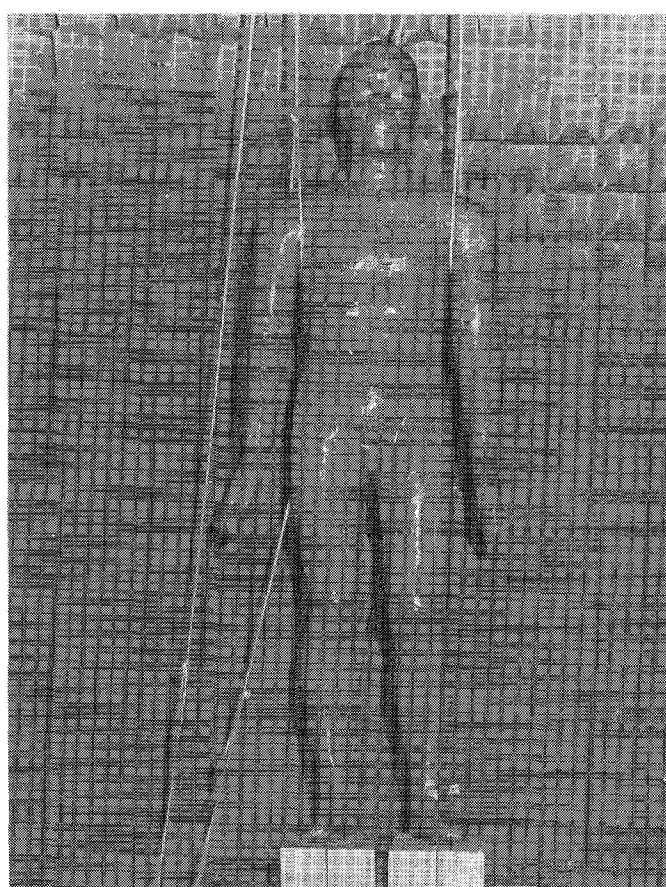


Fig. 3. Suspension of completed phantom man in vertical exposure position in the anechoic chamber.

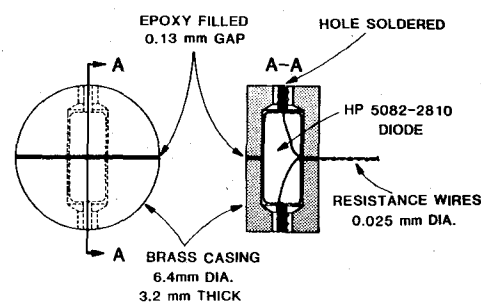
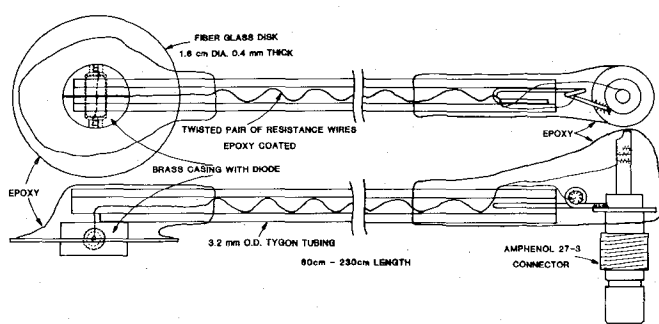


Fig. 4. Construction details of diode electric-field sensor, associated microwave-transparent leads, and coaxial connector.

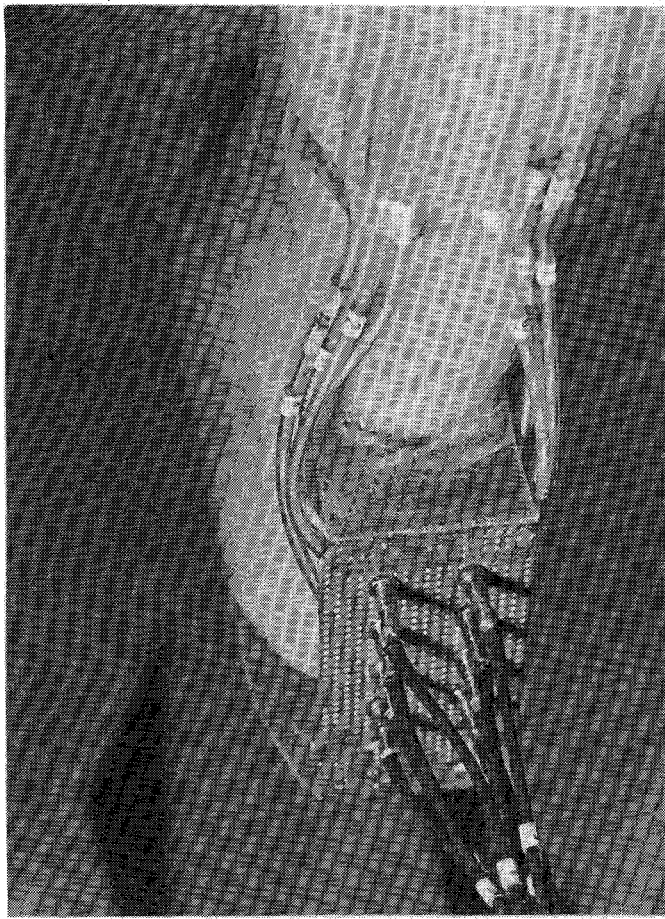


Fig. 5. Signal cable connections to foot of phantom man. The cables strapped to the ankle are the microwave-transparent leads going to the various diode sensors in the model. The signals from these cables are transmitted via coaxial connectors and cables to the instrumentation outside of the anechoic chamber.

instrumentation outside of the shielded room, as shown in Fig. 5. The coaxial cables were kept perpendicular to the  $E$  field and routed away from the back of the man and so were essentially shielded by the body of the model, thereby preventing any serious scattering problems.

Each diode sensor capable of measuring the electric field in the direction of the axis of the diode was encapsulated in a circular disk that would permit its insertion in a predrilled hole through the fiberglass wall of the phantom man but restrict it from going any farther than making a good contact with the surface of the phantom muscle material (Fig. 6). The diode could be rotated in any direction and then fixed in place with masking tape.

#### D. Calibration of Diode Field Detectors

The diode sensors were calibrated under conditions of known incident fields and known SAR by implanting them in a flat-surfaced rectangular phantom-tissue block. The phantom consisted of a box 76 cm  $\times$  76 cm  $\times$  10 cm constructed of 0.3-cm-thick fiberglass walls and filled with synthetic muscle. The slab, with the attached diode sensor, was placed at the exposure position 458 cm in front of the horn in the anechoic chamber. The diode sensor under



Fig. 6. Diode sensor inserted into hole through wall of phantom model, making direct contact with phantom tissue. The sensor may be rotated at any angle with respect to the incident field.

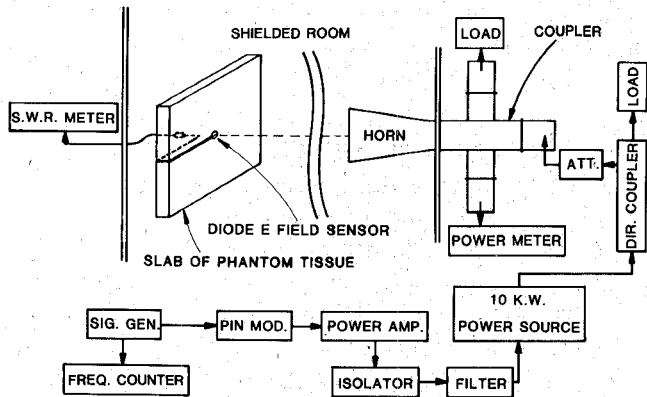


Fig. 7. Schematic of equipment used for calibration of diode electric-field sensors.

calibration was embedded in the synthetic tissue through a precut 6.5-mm-diameter hole in the same manner that it would be inserted into the phantom model man. The sensor was mounted for maximum sensitivity to the vertical electric field at the antenna-boresight line. A schematic diagram of the exposure setup and the connection of the diode to a HP-415E SWR meter for measuring the voltages is shown in Fig. 7. A signal generator was used to drive an intermediate-power amplifier, which in turn was fed through an isolator and filter to a 10-kW klystron power amplifier. The output of the 10-kW amplifier was directed

to a directional coupler into a high-power load, and a sample of the power was taken from the incident arm of the directional coupler for application to the horn in the anechoic chamber. This provided power-density levels within the operating range of the diode sensors mounted on the unclad model man. The signal was modulated with a 1000-Hz square-wave amplifier connected to a pin diode modulator inserted between the signal generator and the power amplifier. The frequency was set to 2450 MHz by means of a frequency counter. Since the HP-VSWR meter is extremely sensitive to 1000-Hz signals, the combination of diode sensor and meter provided a very sensitive field-strength detector.

The diode sensor was first tested to determine whether the small-diameter microwave-transparent leads would cause any interference to the fields or affect the sensor output as a function of lead orientation. A total of 11 diodes were fabricated; ten were used for measurement of the fields at the various locations on the phantom man model, and the 11th was used as a backup. Each diode was calibrated in the rectangular slab.

The diode sensor leads were moved to different angles with respect to the vertically polarized *E* field during exposure of the test slab. Regardless of the angle of the leads, the reading on the HP-415E SWR meter did not vary more than 0.2 dB, indicating that there was negligible field interaction with the leads.

The output voltage as read on a HP-415E VSWR meter in relative units of dB for each of the ten diode *E*-field sensors was obtained for various power densities incident to the flat phantom-tissue slab, with the sensor in electrical contact with the front of the slab. Fig. 8 shows the results of a typical diode, indicating the relationship between the incident power density ( $\mu\text{W}/\text{cm}^2$ ) and the relative meter reading (dB) in the range -30 to -50 dB. All of the diode *E*-field sensors could be reliably used to measure SAR, responding to surface incident power densities as low as  $1 \mu\text{W}/\text{cm}^2$ . The calibration data for all 11 diodes are listed in Table I.

The diode readings were related with the actual SAR's at the surface of the model by measurement of the corresponding rate of temperature rise at each location on the rectangular slab. For this case, the unattenuated output power of the 10-kW source (set for 7 kW) was directed at the slab placed at a distance of 192 cm from the horn in order to rapidly induce a temperature rise at the surface of the slab. The temperature increase versus time was measured with a Vitek-101 probe, with leads transparent to microwave radiation. This information was collected through an analog-to-digital converter and processed by a computer for a printout of temperature versus time.

The SAR values were calculated from the specific heat of the phantom tissue ( $0.86 \text{ kcal}/\text{kg} \cdot ^\circ\text{C}$ ) and the rate of change of temperature with time. The surface SAR was found to be  $0.4 \text{ W}/\text{kg}$  per  $\text{mW}/\text{cm}^2$  incident power density, which is consistent with the theoretical predictions of [5]. The SAR pattern as a function of depth into the muscle slab was also found to be in close agreement with

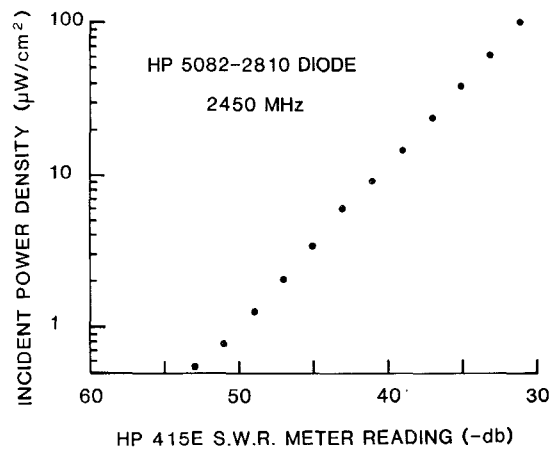


Fig. 8. Typical characteristics of diode *E*-field sensor (no. 1), based on calibration measurements.

theoretical predictions for wave penetration into an exposed semi-infinite tissue medium. This measurement was done to demonstrate that there were no errors due to diode-tissue surface interactions and to verify that the depth dependence of the absorbed energy was the same as for a semi-infinite medium. On the basis of these measurements, a -45-dB reading, for example, from diode number 7 would correspond to  $0.00128 \text{ W}/\text{kg}$ , and a -35-dB reading for the same diode would correspond to  $0.0152 \text{ W}/\text{kg}$ . As seen from Table I, there was considerable variation in the sensitivity of each diode.

#### E. Measurements of Waveguide Transmission Losses of Suit Fabrics

Initial tests of the attenuations of the suits consisted of simple measurements of waveguide transmission loss through the fabric at various locations on the suit. The signal generator was used to transmit a signal through the waveguide to the power meter, where power was noted and compared with the value when the suit was inserted between the flanges of the waveguide. Reflections from the metallized suit were absorbed in the isolator placed between the signal generator and the waveguide adaptor. The attenuation in dB for both parallel (V) and perpendicular (H) polarization with respect to the long axis for all four suits were measured for the fabric at the ten selected locations shown in Fig. 9. The measured results are given in Fig. 10. The results for each individual suit are discussed below.

1) *Wave Guarde Suit*: The measured attenuation of the fabric was found to vary from a minimum of 41 dB to a maximum of 47 dB, as shown in Fig. 10(a). It was not possible to make measurements at the wrist of the suit since the cross-sectional area of the sleeves was insufficient for insertion of the test waveguide.

2) *Milliken Suit*: The attenuation for the fabric of the Milliken suit, shown in Fig. 10(b), varied from a minimum of 23 dB to a maximum of 51 dB. It was not possible to measure the attenuation at the wrist for this suit since, again, the opening was too small or at the head and neck, because a hood was not provided with the suit. In loca-

TABLE I  
CALIBRATION OF DIODE SENSORS IN CONTACT WITH PHANTOM  
MUSCLE AT 2450 MHZ: HP-415E SWR METER READING  
VERSUS INCIDENT POWER DENSITY ( $\mu\text{W}/\text{cm}^2$ )

SWR meter reading (-db)	Diode										
	1	2	3	4	5	6	7	8	9	10	11
24.58											100.4
25											89.3
27											55.8
29											34.7
31											21.6
33	37.86	33.28	65.23	47.47	30.80	68.82	57.68	26.54	19.82	43.05	13.6
35	23.32	20.50	40.24	29.35	18.98	42.45	35.65	16.59	12.41	26.73	8.47
37	14.64	12.80	24.94	18.20	11.90	26.29	22.12	10.30	7.75	16.59	5.29
39	9.15	7.96	15.41	11.41	7.36	16.40	13.80	6.47	4.85	10.39	3.32
41	5.65	4.85	9.62	7.03	4.58	10.03	8.50	4.00	3.06	6.39	2.08
43	3.48	3.00	5.87	4.31	3.32	6.20	5.23	2.47	1.87	3.91	1.28
45	2.33	1.86	3.57	2.65	1.73	3.76	3.13	1.49	1.13	2.38	0.781
47	1.25	1.09	2.04	1.53	1.00	2.26	1.82	0.89	0.69	1.42	0.476
49	0.73	0.63	1.21	0.90	0.58	1.29	1.07	0.51	0.40	0.84	0.281
51											0.163
53											0.099
55											0.060

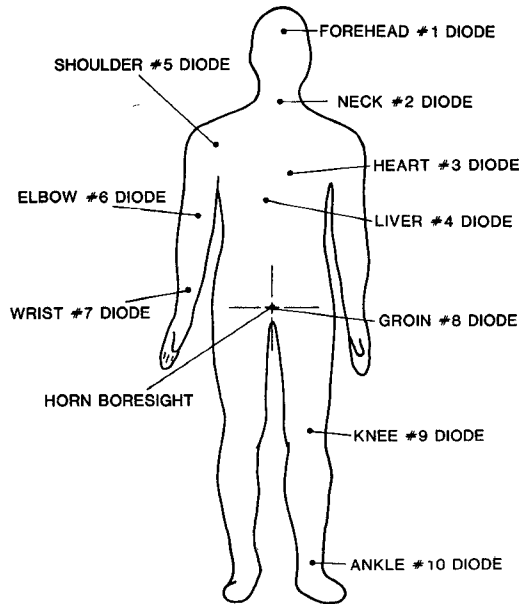


Fig. 9. Schematic of phantom man showing positions where diode electric-field sensors were attached for evaluation of microwave-protective suits.

tions where there was a single layer of suit fabric (at the shoulder, elbow, knee, and ankle), the attenuations were 29 to 36 dB, but in areas where there were double or triple layers of fabric material, such as at the zipper, heart, and groin areas, parallel polarization attenuations were in the range of 45 to 51 dB. The minimum reading of 23 dB using perpendicular polarization for the fabric in the front liver region was probably due to leakage through the nearby zipper.

3) *Invascreen Suit*: The attenuation for this suit fabric was strongly dependent on polarization, as shown in Fig. 10(c). The perpendicular electric-field polarization (15 to 20 dB) was significantly lower than for the parallel polariza-

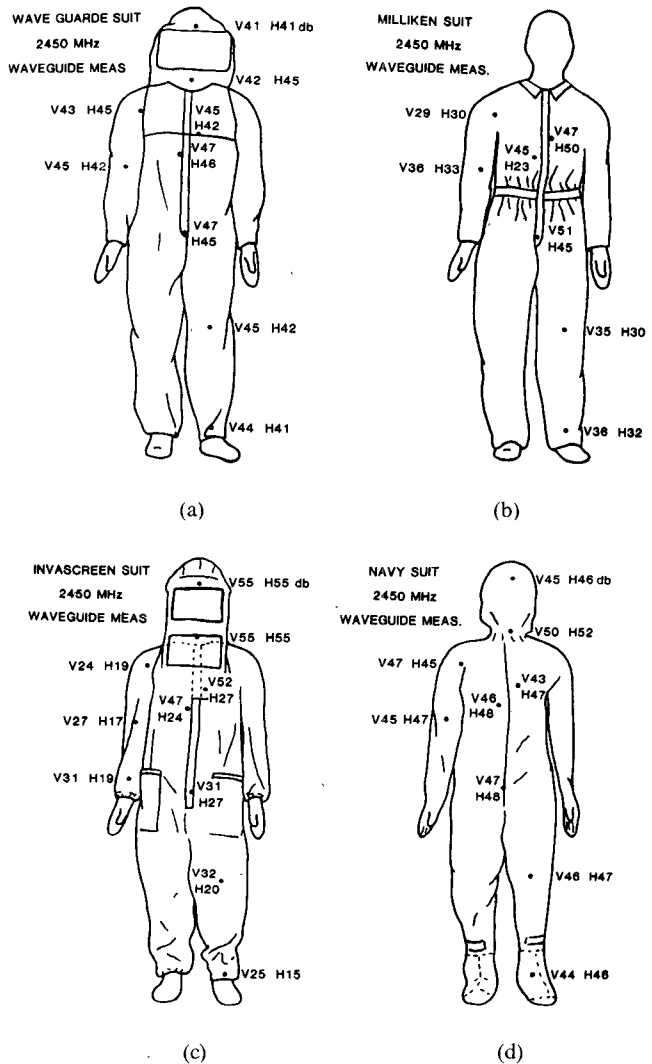


Fig. 10. Results of waveguide-attenuation measurements at various locations on (a) Wave Guarde, (b) Milliken, (c) Invascreen, and (d) U.S. Navy microwave-protective suits. (V indicates values for vertical polarization, and H indicates values for horizontal polarization.)

zation (25 to 31 dB) ( $t$ -test,  $t=7.65$ ,  $df = 4$ ,  $p < 0.002$ ). The attenuations of the fabric at various locations on the front of the body over the heart, liver, and groin were higher because of multiple layers of fabric in the suit's construction. The metal screen material used for fabrication of the hood had an attenuation to 55 dB, much higher than the fabric used for the remainder of the suit.

4) *U.S. Navy Suit*: The attenuation of the fabric for this suit, shown in Fig. 10(d), was the highest, 43 dB at the front, compared with that of the fabric of the other three suits tested. At the zipper in back of the suit, the parallel polarization attenuation was found to be as high as 50 dB, and a perpendicular polarization attenuation as low as 27 dB was found, which is consistent with perpendicular polarization attenuation measured near the zippers on the Milliken and Invascreen suits.

#### F. Exposure of Model with and without Protective Suits to 2450-MHz EM Fields

Ten diode sensors were placed at various locations on the model as shown in Fig. 9, with the diodes oriented for maximum sensitivity in the direction parallel to the long axis of the body. The diodes were inserted through holes on the surface of the model so that they made good contact with the synthetic tissue within. Prior to insertion, each diode was moistened with a saline solution of the same conductivity as the synthetic tissue so as to ensure good electrical contact. The leads from the diodes were carefully routed behind the phantom man and directed toward connectors at the right ankle. Since the U.S. Navy suite was completely closed from head to foot, a seam had to be temporarily opened at the foot to allow exit of the transparent portion of the cables. Miniature coaxial cables carried the signals from the connectors to a switch box and the HP-VSWR meter outside of the chamber. The signals could be quickly switched from various diode locations to the SWR meter.

In a series of experiments, the model was first exposed without the suit on, as shown in the schematic drawing in Fig. 11. For this case, the incident radiation was maintained at relatively low power-density levels by direction of only a portion of the output power of the klystron to the radiating horn via a directional coupler, as shown in the figure. Power density was set so as to provide a reading of either  $-45$  or  $-35$  dB on the standing-wave meter. These values were selected, since they corresponded to the maximum expected reading obtainable with the power source set at maximum power when the body of the phantom man was covered with the suit. These values corresponded to  $3.2$  and  $38 \mu\text{W}/\text{cm}^2$  power density.

For each diode, the input power to the horn corresponding to a  $-45$  or  $-35$  dB reading from each diode was measured, and the incident power density was calculated. The power was then turned off, one of the test suits was placed on the model, and the readings were repeated while a new high input power from the 10-kW amplifier was applied directly to the horn. The power density at the intersection of the boresight line and the man was noted

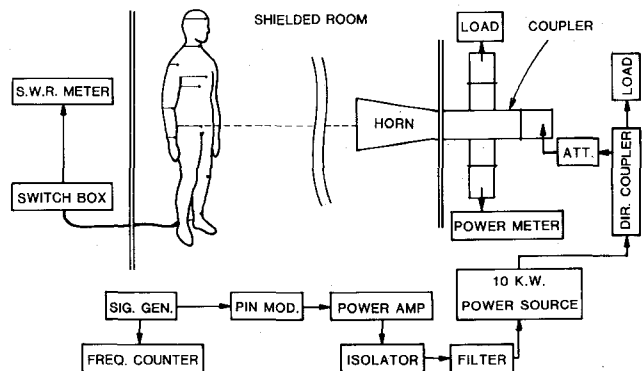


Fig. 11. Schematic drawing of equipment used for exposure of phantom man and measurement of SAR at the surface of the phantom tissue (low power conditions).

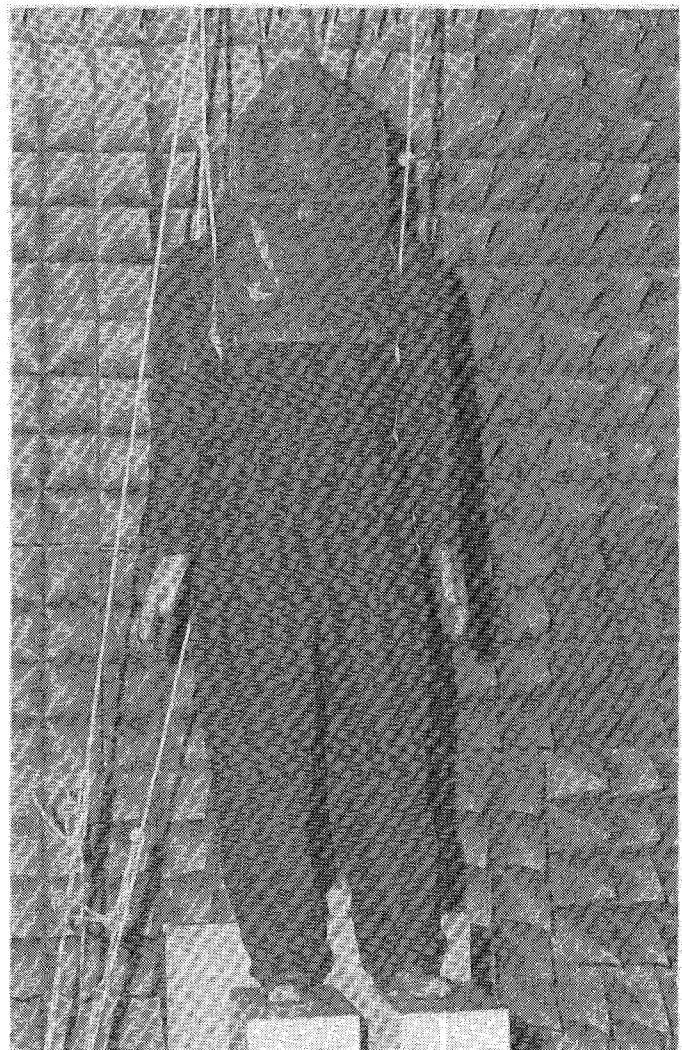


Fig. 12. Phantom man model wearing the Milliken suit (with Wave Guard hood) exposed in vertical position ( $E$  field parallel to body).

based on calibration data obtained previously. Fig. 12 shows the man model exposed in the vertical position while wearing the Milliken suit with  $E$  field parallel to the body.

Diode sensor measurements of body surface  $E$  fields both parallel and perpendicular to the incident  $E$  field

TABLE II  
SPECIFIC ABSORPTION RATES (W/KG PER MW/CM<sup>2</sup> INCIDENT TO MIDSECTION) IN FULL-SIZED MAN EXPOSED TO 2450-MHZ RADIATION

SAR			
	*Due to $E_{pe}$	*Due to $E_{pp}$	Total
EXPOSURE E-FIELD PARALLEL TO LONG AXIS OF BODY			
1**	0.159	$6.34 \times 10^{-4}$	0.160
2	0.153	$4.98 \times 10^{-4}$	0.154
3	0.281	$2.12 \times 10^{-3}$	0.283
4	0.114	$9.54 \times 10^{-4}$	0.134
5	0.099	$7.00 \times 10^{-3}$	0.106
6	0.119	$3.89 \times 10^{-3}$	0.123
7	0.137	$4.17 \times 10^{-3}$	0.137
8	0.152	$4.54 \times 10^{-3}$	0.157
9	0.163	$8.78 \times 10^{-4}$	0.164
10	1.124	$1.81 \times 10^{-2}$	1.142
EXPOSURE E-FIELD PERPENDICULAR TO LONG AXIS OF BODY			
1	0.243	$1.12 \times 10^{-2}$	.254
2	0.124	$2.59 \times 10^{-3}$	.127
3	0.177	$6.96 \times 10^{-3}$	.184
4	0.131	$1.77 \times 10^{-3}$	.133
5	0.089	$2.96 \times 10^{-3}$	.092
6	0.084	$1.18 \times 10^{-2}$	.096
7	0.090	$1.22 \times 10^{-3}$	.091
8	0.056	$3.46 \times 10^{-4}$	.056
9	0.190	$3.81 \times 10^{-3}$	.194
10	0.953	$9.45 \times 10^{-2}$	1.048

\* $E_{pe}$ —E-field component parallel to exposure field;  $E_{pp}$ —E-field component perpendicular to exposure field.

\*\*Numbers refer to locations given in Fig. 9.

were made for all exposures. Exposures were made with the incident  $E$  fields both parallel and perpendicular to the body axis. Localized specific absorption rates were calculated based on the conversion factor of 0.4 W/kg per 1 mW/cm<sup>2</sup> incident power density obtained from the calibration measurements. The SAR values were also normalized to 1 mW/cm<sup>2</sup> at the boresight of the horn, which corresponds to the midpoint of the body near the groin area. Localized tissue surface SAR's calculated from field components both parallel and perpendicular to the long axis of the body, as well as the total SAR obtained from adding the components, are presented in Table II. The data indicate that the electrical field component parallel to the exposure  $E$  field was the major contributor to SAR. The finite electric-field components perpendicular to the exposure  $E$  field may be due in part to scattering or reflection from irregular surfaces of the model and in part to slight misalignment of the diode sensors.

#### G. Attenuation of Suits to Free-Radiation Field

1) *Wave Guarde Suit*: The diode sensor attenuation measurements were first conducted with the Wave Guarde suit on the exposed man model. The calculated SAR's are listed in Table III. The contributions to SAR by  $E$  fields parallel and perpendicular to the long axis of the body are of the same order of magnitude. It appears that the protective suit induces an electric-field component perpendicular to the exposure field, possibly from the anisotropic electrical properties of the fabric. The total SAR values were compared with those for the unclad model in Table II, and the attenuations at the different locations were calculated. These are shown in the last column of Table III and in Fig. 13. The attenuations were reasonably high (21.0–33.7 dB)

TABLE III  
SPECIFIC ABSORPTION RATES (W/KG PER MW/CM<sup>2</sup> INCIDENT TO MIDSECTION) IN FULL-SIZED MAN MODEL WEARING WAVE GUARDE PROTECTIVE SUIT EXPOSED TO 2450-MHZ RADIATION

SAR			
	*Due to $E_{pe}$	*Due to $E_{pp}$	Total
EXPOSURE E-FIELD PARALLEL TO LONG AXIS OF BODY			
1**	$5.62 \times 10^{-4}$	$2.55 \times 10^{-4}$	$8.17 \times 10^{-4}$
2	$1.13 \times 10^{-4}$	$1.04 \times 10^{-5}$	$1.23 \times 10^{-4}$
3	$1.19 \times 10^{-5}$	$5.41 \times 10^{-5}$	$1.73 \times 10^{-4}$
4	$3.76 \times 10^{-5}$	$2.21 \times 10^{-5}$	$5.97 \times 10^{-5}$
5	$2.03 \times 10^{-5}$	$2.51 \times 10^{-5}$	$4.54 \times 10^{-5}$
6	$5.68 \times 10^{-5}$	$2.83 \times 10^{-5}$	$8.51 \times 10^{-5}$
7	$2.53 \times 10^{-5}$	$5.23 \times 10^{-5}$	$3.05 \times 10^{-5}$
8	$4.08 \times 10^{-5}$	$1.49 \times 10^{-5}$	$5.57 \times 10^{-5}$
9	$2.94 \times 10^{-5}$	$2.23 \times 10^{-5}$	$5.17 \times 10^{-5}$
10	$1.52 \times 10^{-2}$	$1.35 \times 10^{-2}$	$2.87 \times 10^{-2}$
EXPOSURE E-FIELD PERPENDICULAR TO LONG AXIS OF BODY			
1	$7.98 \times 10^{-3}$	$1.02 \times 10^{-3}$	$9.00 \times 10^{-3}$
2	$3.58 \times 10^{-4}$	$2.48 \times 10^{-4}$	$6.06 \times 10^{-4}$
3	$4.03 \times 10^{-4}$	$3.93 \times 10^{-4}$	$7.96 \times 10^{-4}$
4	$2.69 \times 10^{-4}$	$3.27 \times 10^{-4}$	$5.96 \times 10^{-4}$
5	$1.02 \times 10^{-4}$	$2.20 \times 10^{-4}$	$3.22 \times 10^{-4}$
6	$1.69 \times 10^{-4}$	$1.80 \times 10^{-4}$	$3.49 \times 10^{-4}$
7	$1.31 \times 10^{-4}$	$2.41 \times 10^{-4}$	$3.72 \times 10^{-4}$
8	$1.07 \times 10^{-4}$	$.449 \times 10^{-5}$	$1.52 \times 10^{-4}$
9	$5.64 \times 10^{-5}$	$4.25 \times 10^{-5}$	$9.89 \times 10^{-5}$
10	$3.62 \times 10^{-3}$	$4.62 \times 10^{-2}$	$4.98 \times 10^{-2}$

\* $E_{pe}$ —E-field component parallel to exposure field;  $E_{pp}$ —E-field component perpendicular to exposure field.

\*\*Numbers refer to locations given in Fig. 9.

for most of the body except at the forehead (14.5 dB) and the ankle (13.2 dB). Thus, based on the measured attenuation and the ANSI Radio Frequency Protection Guide (RFPC) [6] of 5 mW/cm<sup>2</sup>, the whole body would be protected from a maximum exposure of 104 mW/cm<sup>2</sup> when the suit is worn. The low values at the forehead for exposure to perpendicular polarization are probably due to the leakage through the unsealed bottom opening of the hood. The low attenuation at the ankle was caused by leakage through the pants leg opening.

2) *Milliken Suit*: Since the Milliken suit did not have a hood to protect the head, we used the hood from the Wave Guarde suit in testing this suit. The data for these measurements are shown in Table IV and Fig. 13. For the model exposed in a vertical position, the attenuations were 24.3–34.5 dB for various parts of the body, except 20.3 dB at the wrist near the opening of the sleeve of the suit. When the model was placed horizontally, i.e., with body axis perpendicular to the electric field, the attenuations were quite low (2.0–19.2 dB), owing to leakage through the many openings of the suit—the sleeves, trousers, center zipper, neck opening, and two pockets with open sides. The suit would provide protection from maximum exposure levels of 10 mW/cm<sup>2</sup> for the whole body or 48 mW/cm<sup>2</sup> for the body above the ankles.

3) *Invascreen Suit*: This suit was received without the protective gloves and socks, which are indicated as part of the protective system in the company's advertisement brochure. The results of the diode sensor measurements, shown in Table V and Fig. 13, indicate fair (18.7–24.5 dB) attenuation for the parallel polarized  $E$ -field exposure and poor (0.4–21.1 dB) for the perpendicular polarized  $E$  field.

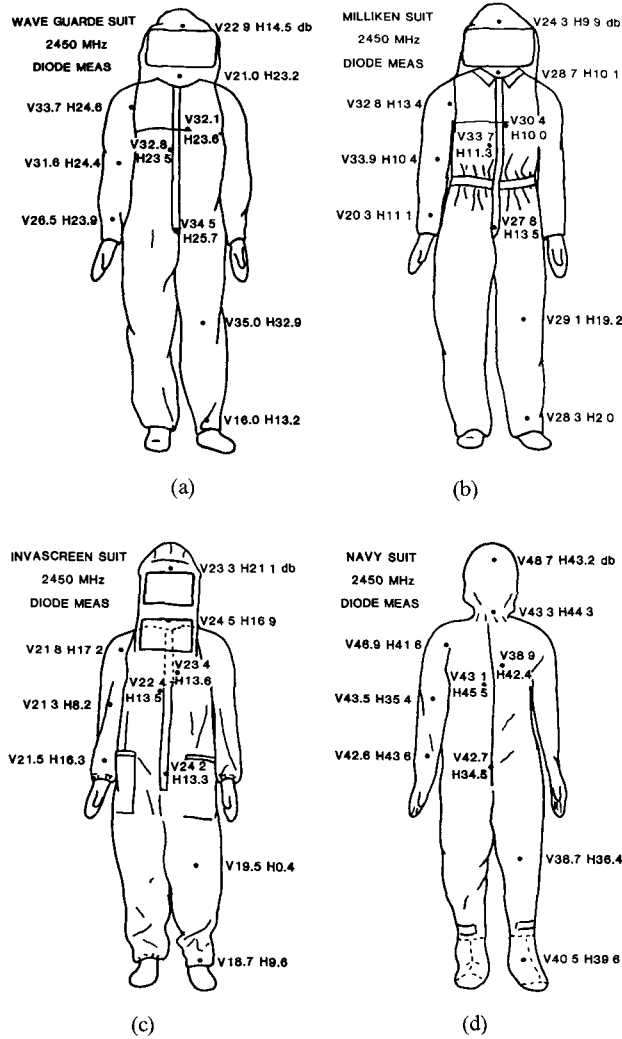


Fig. 13. Values of attenuation of total field (Hermitian magnitude) at body surface protected by (a) Wave Guard, (b) Milliken, (c) Invacreen, and (d) U.S. Navy microwave-protective suit determined from diode electric-field sensors when the suits were exposed to  $E$  fields parallel to body long axis denoted by V and perpendicular to body axis denoted by H.

The 0.4-dB attenuation at the knee is unexplainable. For most parts of the model body, the attenuations obtained by diode measurements were quite consistent with the waveguide measurements; i.e., the attenuations for parallel polarized fields were less than those for perpendicular polarized fields. Although the material is not ideal, this suit is well designed because of the elimination of openings where leakage can occur. Therefore, there was no appreciable change in attenuation for exposure of the model in a horizontal position, as seen in the Milliken suit. The suit would provide no significant protection to the legs at the knees or below, but would protect the rest of the body for a maximum exposure level of  $37 \text{ mW/cm}^2$ .

4) U.S. Navy Suit: This suit provided excellent attenuation (34.5–48.7 dB) for both parallel and perpendicular polarized exposures (see Table VI and Fig. 13). The major reasons for the high attenuation are the high attenuation of the fabric itself (Fig. 10(d)) and the completely closed design of the suit. Based on attenuation only

TABLE IV  
SPECIFIC ABSORPTION RATES (W/KG PER MW/CM<sup>2</sup> INCIDENT TO MIDSECTION) IN FULL-SIZED MAN MODEL WEARING MILLIKEN PROTECTIVE SUIT EXPOSED TO 2450-MHz RADIATION

	SAR			
	*Due to $E_{pe}$	*Due to $E_{pp}$	Total	Suit attenuation (db)
EXPOSURE E-FIELD PARALLEL TO LONG AXIS OF BODY				
1**	$2.16 \times 10^{-4}$	$3.75 \times 10^{-4}$	$5.91 \times 10^{-4}$	24.3
2	$7.07 \times 10^{-5}$	$1.36 \times 10^{-4}$	$2.07 \times 10^{-4}$	28.7
3	$1.04 \times 10^{-4}$	$1.54 \times 10^{-5}$	$2.58 \times 10^{-5}$	30.4
4	$2.19 \times 10^{-5}$	$2.62 \times 10^{-5}$	$4.81 \times 10^{-5}$	33.7
5	$1.38 \times 10^{-5}$	$4.17 \times 10^{-5}$	$5.55 \times 10^{-5}$	32.8
6	$1.19 \times 10^{-4}$	$3.85 \times 10^{-3}$	$5.04 \times 10^{-5}$	33.9
7	$2.02 \times 10^{-4}$	$1.08 \times 10^{-3}$	$1.28 \times 10^{-3}$	20.3
8	$2.38 \times 10^{-4}$	$2.46 \times 10^{-5}$	$2.63 \times 10^{-4}$	27.8
9	$1.72 \times 10^{-4}$	$2.89 \times 10^{-5}$	$2.01 \times 10^{-4}$	29.1
10	$2.55 \times 10^{-4}$	$1.44 \times 10^{-3}$	$1.70 \times 10^{-3}$	28.3
EXPOSURE E-FIELD PERPENDICULAR TO LONG AXIS OF BODY				
1	$2.51 \times 10^{-2}$	$7.24 \times 10^{-4}$	$2.58 \times 10^{-2}$	9.9
2	$1.16 \times 10^{-2}$	$7.18 \times 10^{-3}$	$1.23 \times 10^{-2}$	10.1
3	$1.45 \times 10^{-3}$	$3.78 \times 10^{-3}$	$1.83 \times 10^{-2}$	10.0
4	$8.66 \times 10^{-3}$	$1.32 \times 10^{-3}$	$9.98 \times 10^{-3}$	11.2
5	$3.98 \times 10^{-3}$	$2.22 \times 10^{-3}$	$4.20 \times 10^{-3}$	13.4
6	$7.32 \times 10^{-3}$	$1.43 \times 10^{-3}$	$8.75 \times 10^{-3}$	10.4
7	$3.79 \times 10^{-3}$	$3.31 \times 10^{-3}$	$7.10 \times 10^{-3}$	11.1
8	$2.40 \times 10^{-3}$	$6.85 \times 10^{-5}$	$2.47 \times 10^{-3}$	13.5
9	$2.13 \times 10^{-3}$	$2.03 \times 10^{-4}$	$2.33 \times 10^{-3}$	19.2
10	$6.36 \times 10^{-1}$	$2.71 \times 10^{-2}$	$6.63 \times 10^{-1}$	2.0

\* $E_{pe}$ —E-field component parallel to exposure field;  $E_{pp}$ —E-field component perpendicular to exposure field.

\*\*Numbers refer to locations given in Fig. 9.

TABLE V  
SPECIFIC ABSORPTION RATES (W/KG PER MW/CM<sup>2</sup> INCIDENT TO MIDSECTION) IN FULL-SIZED MAN MODEL WEARING INVACREEN PROTECTIVE SUIT EXPOSED TO 2450-MHz RADIATION

	SAR			
	*Due to $E_{pe}$	*Due to $E_{pp}$	Total	Suit attenuation (db)
EXPOSURE E-FIELD PARALLEL TO LONG AXIS OF BODY				
1**	$7.18 \times 10^{-4}$	$2.82 \times 10^{-5}$	$7.46 \times 10^{-4}$	23.3
2	$5.38 \times 10^{-4}$	$8.48 \times 10^{-5}$	$5.46 \times 10^{-4}$	24.5
3	$1.19 \times 10^{-3}$	$9.15 \times 10^{-5}$	$1.28 \times 10^{-3}$	23.4
4	$6.45 \times 10^{-4}$	$1.53 \times 10^{-5}$	$6.60 \times 10^{-4}$	22.4
5	$6.70 \times 10^{-4}$	$3.23 \times 10^{-5}$	$7.02 \times 10^{-4}$	21.8
6	$7.61 \times 10^{-4}$	$1.44 \times 10^{-4}$	$9.05 \times 10^{-4}$	21.3
7	$9.13 \times 10^{-4}$	$3.36 \times 10^{-5}$	$9.67 \times 10^{-4}$	21.5
8	$5.70 \times 10^{-4}$	$2.41 \times 10^{-5}$	$5.94 \times 10^{-4}$	24.2
9	$1.41 \times 10^{-3}$	$4.29 \times 10^{-4}$	$1.84 \times 10^{-3}$	19.5
10	$1.35 \times 10^{-2}$	$2.02 \times 10^{-3}$	$1.55 \times 10^{-2}$	18.7
EXPOSURE E-FIELD PERPENDICULAR TO LONG AXIS OF BODY				
1	$1.28 \times 10^{-3}$	$6.93 \times 10^{-4}$	$1.97 \times 10^{-3}$	21.1
2	$1.63 \times 10^{-3}$	$9.52 \times 10^{-4}$	$2.58 \times 10^{-3}$	16.9
3	$6.85 \times 10^{-4}$	$7.36 \times 10^{-3}$	$8.05 \times 10^{-3}$	13.6
4	$5.23 \times 10^{-3}$	$6.94 \times 10^{-4}$	$5.92 \times 10^{-3}$	13.5
5	$1.40 \times 10^{-3}$	$3.60 \times 10^{-3}$	$1.76 \times 10^{-3}$	17.2
6	$5.58 \times 10^{-3}$	$8.84 \times 10^{-3}$	$1.44 \times 10^{-2}$	8.2
7	$1.76 \times 10^{-3}$	$3.65 \times 10^{-4}$	$2.13 \times 10^{-3}$	16.3
8	$2.38 \times 10^{-3}$	$2.28 \times 10^{-3}$	$2.61 \times 10^{-3}$	13.3
9	$1.75 \times 10^{-1}$	$2.32 \times 10^{-3}$	$1.77 \times 10^{-1}$	0.4
10	$9.94 \times 10^{-3}$	$1.05 \times 10^{-1}$	$1.15 \times 10^{-1}$	9.6

\* $E_{pe}$ —E-field component parallel to exposure field;  $E_{pp}$ —E-field component perpendicular to exposure field.

\*\*Numbers refer to locations given in Fig. 9.

and discounting voltage breakdown or fire hazards, the suit would provide protection to exposure levels up to  $14\,000 \text{ mW/cm}^2$ .

#### H. Exposure Tests of Protective Suit Fabrics to High-Power Waveguide Fields

It was found from simple open-flame tests on small fabric pieces cut from the pocket facing from each suit that

TABLE VI  
SPECIFIC ABSORPTION RATES (W/KG PER MW/CM<sup>2</sup> INCIDENT TO  
MIDSECTION) IN FULL-SIZED MAN MODEL WEARING U.S. NAVY  
PROTECTIVE SUIT EXPOSED TO 2450-MHz RADIATION

	SAR			
	*Due to $E_{pe}$	*Due to $E_{pp}$	Total	Suit attenuation (dB)
EXPOSURE E-FIELD PARALLEL TO LONG AXIS OF BODY				
1**	$1.84 \times 10^{-6}$	$3.20 \times 10^{-7}$	$2.16 \times 10^{-6}$	48.7
2	$6.64 \times 10^{-6}$	$4.89 \times 10^{-7}$	$7.13 \times 10^{-6}$	43.3
3	$3.56 \times 10^{-5}$	$1.00 \times 10^{-6}$	$3.66 \times 10^{-5}$	38.9
4	$4.79 \times 10^{-6}$	$7.28 \times 10^{-7}$	$5.52 \times 10^{-6}$	43.1
5	$1.76 \times 10^{-6}$	$3.86 \times 10^{-7}$	$2.15 \times 10^{-6}$	46.9
6	$3.27 \times 10^{-6}$	$2.28 \times 10^{-6}$	$5.55 \times 10^{-6}$	43.5
7	$7.01 \times 10^{-6}$	$5.29 \times 10^{-7}$	$7.54 \times 10^{-6}$	42.6
8	$6.16 \times 10^{-6}$	$2.28 \times 10^{-6}$	$8.44 \times 10^{-6}$	42.7
9	$2.17 \times 10^{-5}$	$5.46 \times 10^{-7}$	$2.22 \times 10^{-5}$	38.7
10	$5.94 \times 10^{-5}$	$4.17 \times 10^{-5}$	$1.01 \times 10^{-4}$	40.5
EXPOSURE E-FIELD PERPENDICULAR TO LONG AXIS OF BODY				
1	$2.34 \times 10^{-6}$	$9.87 \times 10^{-6}$	$1.22 \times 10^{-5}$	43.2
2	$3.50 \times 10^{-6}$	$1.17 \times 10^{-6}$	$4.67 \times 10^{-6}$	44.3
3	$8.96 \times 10^{-6}$	$1.61 \times 10^{-6}$	$1.06 \times 10^{-5}$	42.4
4	$2.70 \times 10^{-6}$	$1.04 \times 10^{-7}$	$3.74 \times 10^{-6}$	45.5
5	$5.36 \times 10^{-6}$	$9.50 \times 10^{-7}$	$6.31 \times 10^{-6}$	41.6
6	$5.29 \times 10^{-6}$	$2.24 \times 10^{-6}$	$2.77 \times 10^{-5}$	35.4
7	$2.44 \times 10^{-6}$	$1.51 \times 10^{-7}$	$3.95 \times 10^{-6}$	43.6
8	$1.88 \times 10^{-5}$	$8.52 \times 10^{-7}$	$1.97 \times 10^{-5}$	34.5
9	$3.57 \times 10^{-5}$	$8.81 \times 10^{-6}$	$4.45 \times 10^{-5}$	36.4
10	$1.66 \times 10^{-4}$	$9.94 \times 10^{-5}$	$1.16 \times 10^{-4}$	39.6

\* $E_{pe}$ —E-field component parallel to exposure field;  $E_{pp}$ —E-field component perpendicular to exposure field.

\*\*Numbers refer to locations given in Fig. 9.

both the Wave Guarde and the U.S. Navy suit fabrics were very flammable, the Invascreen suit fabric was less flammable, and the Milliken suit was resistant to flame. Thus, to reduce the fire hazard, only the Milliken suit was exposed to high incident power. The fabric of the suit was placed in the same waveguide setup used for the attenuation measurements but with higher input power, 59 W, applied for 1 h over a 59-cm<sup>2</sup> WR-430 waveguide aperture at the load junction. This corresponded to 1000 mW/cm<sup>2</sup> average, or 2000 mW/cm<sup>2</sup> peak, power density at the center of the waveguide.

### III. CONCLUSIONS

The performance of four microwave-protective suits: the Wave Guarde (AT&T), Milliken, Invascreen, and U.S. Navy suits was tested. Using the waveguide-transmission-loss test, both the Wave Guarde and the U.S. Navy suit fabrics were found to provide at least 40-dB attenuation. The Milliken material provided at least 30-dB attenuation independent of fabric orientation. The attenuation of the Invascreen material was quite poor, showing an orientation dependence from 17–19 dB for perpendicular polarized E-field exposure to 24–32 dB for parallel polarized E-field exposure.

Since the waveguide method provides only a comparison between the attenuations of various fabrics and does not evaluate the other factors, such as seams and overall suit design, that affect shielding properties, the suits were put on a full-sized man model filled with phantom muscle, and tests with ten diode E-field sensors were conducted. The attenuations at the forehead, neck, heart, liver, shoulder, elbow, wrist, groin, knee, and ankle were calculated by comparison of two sets of diode sensor readings, one taken

with and one taken without the suits on the exposed model.

The Wave Guarde suit provided attenuations between 20 and 35 dB for most parts of the body. A few low attenuation values (13.2–16 dB) were obtained at locations on the head and ankle owing to the open head hood and the opening of the pant leg at the ankle. The Milliken suit (with the Wave Guarde hood) provided quite good attenuation (20–35 dB) for parallel electrical-field exposure, but low attenuation (2–19 dB) for perpendicular polarized field exposure owing to the poor design (multiple openings) of the suit. The Invascreen suit was well designed to prevent leakage; however, the intrinsic poor attenuation of the fabric material resulted in poor shielding (18.7–24.5 dB for parallel E field of exposure and 0.4–21.1 dB for perpendicular E-field exposure). The highest attenuation was provided by the Navy suit, which had a range of 34.5 to 48.7 dB for exposures in both the parallel and perpendicular orientations with respect to the E Field. This effective shielding is due to the complete enclosure of the man inside the suit and minimal fabric openings.

Therefore, in terms of shielding effectiveness, the Navy suit was the best, the Wave Guarde was the second best, and the Milliken and Invascreen were the least effective. However, the flammability of the Navy and Wave Guarde suits presents a fire risk. Open-flame tests indicated that the Milliken fabric material is the most fire retardant.

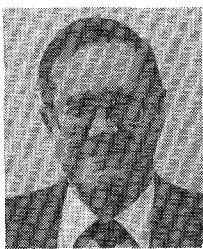
An ideal combination would be the high attenuation and the minimal-opening design of the Navy suit and the fire-retardant properties of the Milliken fabric. An adequate compromise would be to tailor a suit of the Navy design with Milliken material; such a suit should pose no fire hazard and provide at least a 30-dB attenuation.

### ACKNOWLEDGMENT

The authors thank R. Peterson, of Bell Laboratories, for his guidance and Dr. E. Postow, National Naval Medical Center, Bethesda, MD, for providing the U.S. Navy suit.

### REFERENCES

- [1] Z. R. Glaser and G. M. Heimer, "Determination and elimination of hazardous microwave fields aboard Naval ships," *IEEE Trans. Microwave Theory Tech.*, vol. MTT-19, pp. 232–238, Feb. 1971.
- [2] B. A. Minin, *Microwaves and Human Safety—Part 2*. Moscow: Izdatel'stvo Sovetskoye Radio, 1974 (Transl. by Joint Publications Research Service, JPRS 65506-2, pp. 279–292, 1975).
- [3] A. W. Guy, "Analyses of electromagnetic fields induced in biological tissues by thermographic studies on equivalent phantom models," *IEEE Trans. Microwave Theory Tech.*, vol. MTT-19, pp. 205–214, Feb. 1971.
- [4] A. W. Guy, C. K. Chou, C. Sorenson, J. A. McDougall, G. Y. Yang, and D. Reynolds, "Specific absorption rates of energy in man models exposed to UHF-mobile antenna fields," *IEEE Trans. Microwave Theory Tech.*, vol. MTT-34, pp. 671–680, June 1986.
- [5] C. C. Johnson and A. W. Guy, "Nonionizing electromagnetic wave effects in biological materials and systems," *Proc. IEEE*, vol. 60, no. 6 pp. 692–718, 1972.
- [6] ANSI C95.1-1982, "Safety levels with respect to human exposure to radiofrequency electromagnetic fields, 300 kHz to 100 GHz," Radiofrequency Protection Guide, 1982.



**Arthur W. Guy** (S'54–M'57–SM'74–F'77) was born in Helena, MT, on December 10, 1928. He received the B.S. degree in 1955, the M.S. degree in 1957, and the Ph.D. degree in 1966, all in electrical engineering, from the University of Washington, Seattle.

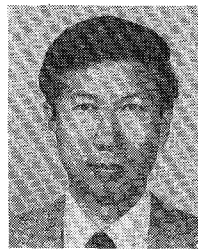
From 1947 to 1950 and from 1951 to 1952, he served in the U.S. Air Force as an Electronics Technician. Between 1957 and 1964 he was a Research Engineer in the Antenna Research Group, Boeing Aerospace Company, Seattle.

While there, his field included research on broad-band and microwave devices, surface wave antennas, propagation through anisotropic dielectrics, and antennas buried in lossy media. Between 1964 and 1966 he was employed by the Department of Electrical Engineering, University of Washington, conducting research on VLF antennas buried in polar ice caps. At that time, he also served as Consultant to the Department of Rehabilitation Medicine, working on problems associated with the effect of electromagnetic fields on living tissue. In 1966, Dr. Guy joined the faculty in the Department of Rehabilitation Medicine. Presently, he is a Professor in the Center for Bioengineering, with a joint appointment as Professor in Rehabilitation Medicine and Adjunct Professor in Electrical Engineering. He is Director of the Bioelectromagnetics Research Laboratory in the Bioengineering Center and is involved in teaching and research in the area of biological effects and medical applications of electromagnetic energy.

Dr. Guy is a member of the AAAS, Bioelectromagnetics Society, the IEEE ANSI C95 Committee, ANSI C95.4 Subcommittee, and was Chairman of the 1970–1982 Subcommittee IV that developed the protection guides for human exposures to radio-frequency fields in 1974 and 1982. He is a member of NCRP, and Chairman of the Scientific Committee 53 responsible for biological effects and exposure criteria for radio-frequency fields, Chairman Elect of the IEEE Committee of Man and Radiation (COMAR), member of the U.S. National Committee of URSI Commission A, and past member of the EPA Scientific Advisory Board Ad Hoc Committee on Biological Effects of Radiofrequency Fields. Dr. Guy also serves as a consultant of the NIEHS on the USSR-US Environmental Health Cooperative Program and was a member of the NIH Diagnostic Radiology Study Section 1979–1983. Dr. Guy is a member of the editorial boards of the *Journal of Microwave Power* and IEEE TRANSACTIONS ON MICROWAVE THEORY AND TECHNIQUES and is Past-President of the Bioelectromagnetics Society. Dr. Guy holds memberships in Phi Beta Kappa, Tau Beta Pi, and Sigma Xi.



**Chung-Kwang Chou** (S'72–M'75–SM'86) was born in Chung-King, China, on May 11, 1947.



He received the B.S. degree from National Taiwan University in 1968, the M.S. degree from Washington University, St. Louis, MO, in 1971, and the Ph.D. degree from the University of Washington, Seattle, in 1975, all in electrical engineering.

During his graduate study at the University of Washington, Dr. Chou had extensive training in both electromagnetics and physiology. He spent a year as a NIH postdoctoral fellow in the Regional Primate Research Center and the Department of Physiology and Biophysics at the University of Washington. He was a Research Associate Professor in the Center for Bioengineering and the Department of Rehabilitation Medicine, as well as Associate Director of the Bioelectromagnetics Research Laboratory until August 1985 engaged in teaching and research in electromagnetic dosimetry, exposure systems, biological effects of microwave exposure, and RF hyperthermia for cancer treatment. He is now the head of the Biomedical Engineering Section and the Associate Director of the Department of Radiation Research at the City of Hope National Medical Center, Duarte, CA. His main research there is in cancer hyperthermia. A consultant for the NCRP's scientific committee 53 on the biological effects and exposure criteria for radio-frequency electromagnetic fields, Dr. Chou has also served on the ANSI Subcommittee C95.4 since 1978, and is the Chairman of the 3 kHz–3MHz working group. He was the Chapter Chairman of IEEE's Seattle Section on Antennas and Propagation/Microwave Theory and Technique in 1981–1982. Dr. Chou was on the Board of Directors of the Bioelectromagnetics Society and is now the Associate Editor of the *Journal of Bioelectromagnetics*. He is also a member of the Bioelectromagnetics peer review group of the American Institute of Biological Sciences.

In 1981, Dr. Chou received the Special Award for the Decade of the 1970's for contributions in medical and biological research and in 1985 the Outstanding Paper Award, both from the International Microwave Power Institute. Dr. Chou is a member of BEMS, AAAS, IMPI, the Radiation Research Society, North American Hyperthermia Group, Tau Beta Pi and Sigma Xi.



**John A. McDougall** (M'87), photograph and biography not available at the time of publication.



**Carrol Sorensen**, photograph and biography not available at the time of publication.